Original Article

A Cost-effective Breath-hold Coaching Camera System for Patients Undergoing External Beam Radiotherapy

Akash Mehta, Emma Horgan, Prabhakar Ramachandran, Christopher Noble
Department of Radiation Oncology, Princess Alexandra Hospital, Woolloongabba, Australia

Abstract

Purpose: Organ motion can significantly affect the accurate delivery of radiation doses to the tumor, particularly for sites such as the breast, lung, abdomen, and pelvis. Managing this motion during treatment is crucial. One strategy employed to manage motion induced from respiration is breath-hold (BH), which enhances the geometric precision of dose delivery. Our institute is transitioning to using the ExacTrac Dynamic system to facilitate patient BH using surface-guided cameras. Only 20% of our linacs are equipped with surface guidance capabilities, and due to a high patient stereotactic throughput, the ability to perform in-bunker coaching for BH patients within the bunker is limited. To address this challenge, a time-of-flight camera (ToF) was developed to coach radiotherapy patients undergoing BH procedures, allowing them to gain confidence in the process outside of the bunker and before treatment. **Methods:** The camera underwent testing for absolute and relative accuracy, responsiveness under various environmental conditions, and comparison with the Elekta Active Breathing Coordinator (ABC) to establish correlation and testing on volunteers independently to assess usability. **Results:** The results showed that the absolute distance measured by the camera was nonlinear due to square light modulation, which was retrospectively corrected. Relative accuracy was tested with a QUASAR motion phantom, with results agreeing to within ± 2 mm. The camera response was found to be unaffected by changes in lighting or temperature, though it overresponded under extreme temperatures. The comparison with the Elekta ABC system yielded comparable results between lung volume and changes in surface distance during BH. All volunteers successfully followed instructions and maintained BH within ± 1 mm tolerance. **Conclusions:** This study demonstrates the feasibility of using a cost-effective ToF camera to coach patients before imaging/treatment, saving valuable LINAC linac and imaging system time.

Keywords: ArduCam®, breath-hold, ExacTrac Dynamic®, raspberry pi, time-of-flight camera

Received on: 13-06-2024 **Review completed on:** 18-08-2024 **Accepted on:** 13-11-2024 **Published on:** 18-12-2024

Introduction

Advancements in radiation oncology treatment delivery techniques such as volumetric modulated arc therapy (VMAT) and stereotactic body radiation therapy, allow high precision of radiation delivery to the tumor while minimizing dose to normal tissues and organs at risk. These treatments require precise patient setup to mitigate inaccuracies in dose delivery. To account for this, image-guided radiotherapy facilitates the alignment of patients to planned treatment positions. In addition to this, internal organ motion can also alter the intended dose delivery to the tumor, particularly, in sites such as the breast, lung, or abdomen, if not managed during the treatment. There are a number of strategies that are available to improve the geometrical accuracy of dose delivery by minimizing or accounting for the internal organ motion, which includes the use of an abdominal compression belt, four-dimensional computed tomography (CT) planning, respiratory gating, and breath-hold (BH).[1,2]

BH conditions are generally facilitated using respiration monitoring tools, which allow the patient to reproduce the BH with high accuracy during both simulation and treatment. The monitoring tools may include spirometers (e.g. Active Breathing Coordinator™ [ABC][3]), a real-time patient positioning system (Varian RPM™[4]), laser and camera-based monitoring systems,[5] high-resolution surface imaging cameras employed for surface-guided radiation therapy (SGRT)

Access this article online

Quick Response Code:

Website: www.jmp.org.in

DOI: 10.4103/jmp.jmp_101_24

Address for correspondence: Dr. Christopher Noble, Department of Radiation Oncology, Princess Alexandra Hospital, Woolloongabba QLD 4102, Australia.
E-mail: christopher.noble@health.qld.gov.au

This is an open access journal, and articles are distributed under the terms of the Creative Commons Attribution-NonCommercial-ShareAlike 4.0 License, which allows others to remix, tweak, and build upon the work non-commercially, as long as appropriate credit is given and the new creations are licensed under the identical terms.

For reprints contact: WKHLRPMedknow_reprints@wolterskluwer.com

How to cite this article: Mehta A, Horgan E, Ramachandran P, Noble C. A cost-effective breath-hold coaching camera system for patients undergoing external beam radiotherapy. J Med Phys 2024;49:502-9.

systems such as Align-RT,[6] C-RAD,[7] Identify,[8] and ExacTrac Dynamic systems.[9,10]

SGRT systems are widely used in radiotherapy to enhance the accuracy of patient positioning and motion monitoring during treatment. They provide real-time feedback on patient positioning, motion, and intra-fractional changes. They rely on the use of cameras or depth sensors to capture the patient's surface information in real time, allowing for precise alignment and tracking of the treatment area.[11]

A number of different types of surface-guided cameras are used in radiotherapy such as structured light cameras, stereo vision cameras, depth-sensing cameras, and time-of-flight (ToF) cameras. Stereo vision systems use two or more cameras to capture images of the patient's surface from different angles. By analyzing the disparity between the images, the system can reconstruct the three-dimensional (3D) surface information. This allows for accurate tracking of patient motion and verification of the treatment position.[12]

Structured light cameras utilize structured light patterns projected onto the patient's skin. These cameras capture the reflected light, and based on the distortion of the projected pattern, the system calculates the 3D surface information of the patient. The acquired data are then compared against a reference surface from the treatment planning datasets to determine the patient's position.[13]

Depth sensing systems employ sensors, such as ToF cameras or structured light cameras[14] with depth sensing capabilities, to directly measure the distance between the camera and the patient's surface.The depth information is used to create a 3D representation of the patient's surface, enabling precise monitoring, and positioning during radiotherapy. ToF cameras typically consist of an emitter, which emits a modulated infrared light signal (~850 nm), and a receiver, which captures the reflected light and converts the photon energy to electrical current. The camera calculates the depth information based on the time it takes for the emitted light to return to the camera sensor. By combining this depth information with the camera's traditional two-dimensional image sensor, ToF cameras can provide color-coded depth data to provide the user a better visual experience,[15] e.g. blue color can be chosen to display objects far away, and red for closer objects.

ToF cameras can be further divided into direct ToF (dToF) and continuous wave ToF. The continuous wave method uses a square wave or sinusoidal modulated light source, typically a vertical-cavity surface-emitting laser (VCSEL) diode. The reflected light from the object is detected with an IR detector array which is gated at the modulation frequency of the light source at four different phases. This results in an image formed using each of the four phases. These images can then be processed to obtain a depth map using the following equation. Note that equation 1 assumes sinusoidal modulation.[15]

$$d = \frac{c}{4\pi f} tan^{-1} \frac{\Phi_3 - \Phi_4}{\Phi_1 - \Phi_2} \quad \text{..... equation 1}$$

In addition to this, the pixel intensity (A) of the final image can also be calculated using the equation 2:

$$A = \frac{\sqrt{(\Phi_1 - \Phi_2)^2 + (\Phi_3 - \Phi_4)^2}}{2} \quad \text{..... equation 2}$$

where,

A is the pixel intensity

c is the speed of light

f is the modulation frequency

Φ_1, Φ_2, Φ_3, and Φ_4 represent the electrical charges accumulated at different capacitance levels as shown in Figure 1.

dToF cameras such as those used in automotive applications and some smartphones use pulsed light rather than continuous modulated light and use time-to-digital converters and histogram builders for each pixel in the detector array to directly determine the time of flight for the reflected light and hence distance. The light source for the camera is typically an array of VCSELs and the detectors in the array are typically single-photon avalanche diodes.[16]

At our institution, Elekta's ABC system is currently used for the treatment of breast, liver, and lung cancers in BH conditions. It allows patients to maintain a reproducible BH condition either in end-expiration or end-inspiration phase for aiding to minimize the internal organ movements. The ABC system consists of a balloon valve that inflates during BH preventing the airflow through the spirometer and deflates upon triggering the patient control switch or at the completion of the BH cycle.[3] The spirometer measures the volume of the air intake during the inhale phase and the change in the volume during the exhale stage.

In addition to the use of ABC for BH treatments, the department is investigating using the existing Exactrac Dynamic system for VMAT breast cancer patients requiring BH. The Exactrac Dynamic system combines thermal information with the surface grid to provide highly accurate tracking of the patient's surface throughout the delivery. It also allows the patients to observe their breath pattern and optimal BH position by providing live feedback during the treatment. BH is patient-specific and requires coaching to match the treatment setup configuration. Due to the large throughput of stereotactic patients on our linac with Exactrac Dynamic, we are limited with how much time is available to coach patients for ExacTrac Dynamic treatments. Therefore, in this study, we propose an alternative BH coaching method, which was developed using an in-house low-cost ToF camera modeling the ExacTrac Dynamic interface.

Methods

The in-house ToF camera (addressed hereafter as ToF camera or camera) system consists of a Wi-Fi-compatible Raspberry Pi 3B with an Arducam ToF camera connected and placed in a Raspberry Pi case. It requires a 5V 4A power supply and

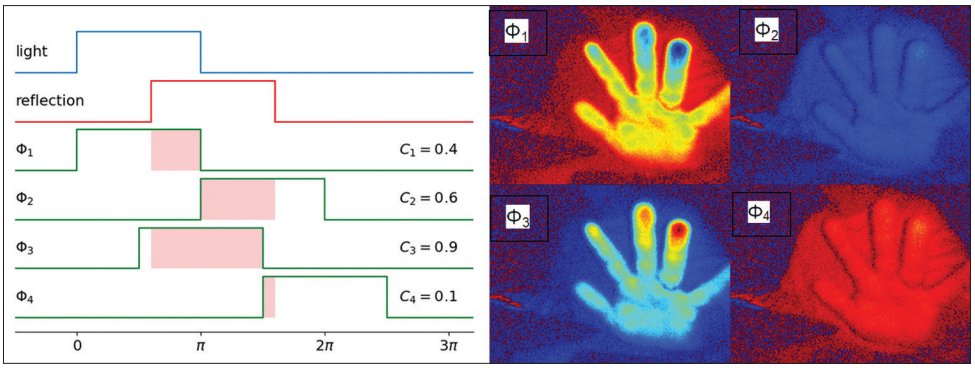

Figure 1: The emitted light (in blue), reflected light (in red), four phases each sampled at 90° apart; Φ_1, Φ_2, Φ_3, and Φ_4 represent the electrical charges accumulated during these samples. C_1, C_2, C_3, and C_4 show the intensity in each phase (left); corresponding pixel intensities for each sample (right)

can be attached to a phone tablet holder for positioning. The JavaScript-coded system operates on *Raspbian Bullseye* OS and uses ArduCAM libraries in the backend. The ToF camera has a continuous-wave (CW) light source, in which the light is emitted in square waveforms. The CW method accepts four samples per measurement and each sample has a phase shift of 90° as shown in Figure 1. This allows us to calculate the distance (between the ToF camera and the object) and the phase relation between the emitted and reflected light.[1]

The interface includes an operator view (accessible via a laptop) and a patient view to allow them to observe the breathing pattern. The operator view includes live camera output with a region of interest (ROI) selected for observation. It also displays relative and absolute distance as well as BH target distance, tolerance, ROI radius, and smoothing parameters to cancel out noise. In addition to this, the breathing pattern can be recorded, and a baseline can be established as required. In the patient's view, one sees a simple hovering circle, representing their live surface position with respect to the target position, which allows them to breathe and hold breath accordingly.

Before the utilization of the software for the BH study, a number of tests were performed to assess the functionality of the ToF camera in terms of its response and reliability with the current BH setup. In addition to this, the system was also tested and operated by multiple users to check the performance abilities and ease of use from patients' perceptive.

Absolute accuracy

The absolute distance measurements were conducted to assess the ability of the ToF camera to accurately measure the distance of the camera to the patient within an accepted tolerance. This is important in deciding how far the camera should be positioned for optimal BH results that are reproducible during coaching.

A flat surface was positioned at known distances from the camera in the range of 200 mm to 1200 mm, to perform an absolute distance calibration. A flat surface was chosen to minimize uncertainties caused by pixel averaging, where the pixels inside the ROI are averaged depending on their respective distances from the camera. As far as the patient anatomy is concerned, the aim is to train BH patients for lung and breast cancer patients, for which sternum is the ROI that is mostly flat in nature.

The range of measurements was based on the manufacturer's specification of the nominal range of the camera being 2 m. The anticipated camera position for BH surface tracking was decided to be within 1 m from the patient's surface. For absolute distance accuracy, the measurements were performed up to 1.2 m to observe any further trends.

These measurements were performed in two ways – (1) The camera was positioned in front of the flat surface and a ruler was placed beside the surface. By keeping the ToF camera and ruler stationary, the flat surface was moved by known distances; (2) the flat surface was positioned on a calibrated and tested LINAC couch, and the couch was moved longitudinally by known distances as shown in Figure 2. The second method was used to eliminate any dependency on the flat surface tilt when it was moved manually in method 1. The distance measured by the camera was compared against the actual distance.

For these tests, the potential uncertainty with the couch is ±2 mm (couch tolerance). With the ruler, the uncertainties include zero error, incorrect positioning of the ruler, and parallax error. As the least count on the ruler used was 1 mm, the error would be ±0.5 mm in this case.

Relative accuracy

Once the optimal absolute distance range was decided, it was normalized to the initial position of the ROI in question, and relative measurements were used for generating respiratory patterns. The optimal distance was considered by taking into account the camera position from a patient's perspective, i.e., it should not be too close to the patient for setup purposes.

The Quasar respiratory motion phantom was used to validate the accuracy of the camera's ability to trace the ROI movement as demonstrated in Figure 3. The phantom was positioned at 30 and 40 cm away from the camera and multiple motion amplitudes were traced for a selected ROI. The initial decision to use these distances was based on the volunteer's comfort and considering patient setup procedures, which might involve

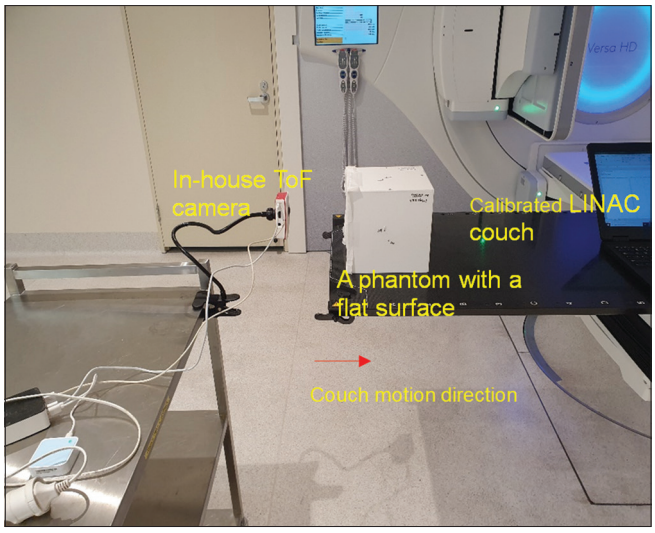

Figure 2: The time-of-flight camera setup for absolute calibration

fine adjustments postinitial setup. If the camera is positioned too close to the patient, there is a possibility of obstructing the positioning process, and could potentially be claustrophobic to some patients. In addition to this, multiple tests were performed which led to the adoption of 40 cm as the optimal distance. This was also performed with a phantom placed with a 5^0 tilt and offset from the camera's central axis.

A ruler was used to preposition the QUASAR phantom with respect to the camera. The placement of the phantom was confirmed with the measurement readings obtained from our calibrated TOF camera. In addition to this, a 5° tilt, and an offset to the extreme position of the camera field-of-view with respect to the TOF camera centerline was used in this study. This was to investigate the impact of subject positioning on breathing traces/measurements and establish a correlation between patient position and the centerline of the camera.

The test was aimed at checking the functionality of the camera and its ability to respond to ROI motion. The intended use of the camera is to coach BH patients; the fast acceleration would have been out of scope for this purpose. In addition to this, normal respiration rates for an adult person at rest range from 12 to 16 bpm. Based on these assumptions, 15 bpm was used.

Response under different conditions

The main goal of developing this camera was to establish a system that can be used in a patient examination or a mold room (i.e., designated areas other than LINACs or CTs) preserving the treatment time on linacs or CT scanners. Since the camera is designed to be used in multiple locations, it was important to investigate the effect of variable lighting setups, temperature, and/or training duration. Therefore, the camera was tested under different setup conditions to investigate its behavior.

Different light arrangements were used to measure the distance of an object from the camera. In addition to this, its temperature dependency was tested using a heat gun (which can go up

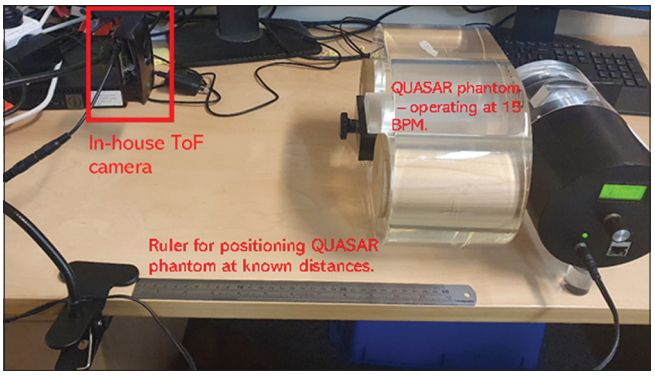

Figure 3: The relative measurements setup with calibrated QUASAR phantom. TOF: Time-of-flight

to ~100°C). The gun was directly aimed at the camera setup and its response before, after, and during the heat was recorded. For long-term stability, the camera was left on for 10 min and its response was noted.

Comparison with Elekta's active breathing coordinator

The ToF camera was tested on 5 volunteers to simulate their BH pattern using an ROI around their sternum area. These volunteers underwent BH using the ABC system and ToF camera simultaneously. This test was performed to correlate these two systems and to test the reproducibility of the camera while maintaining a constant BH with ABC.

Breath-hold tests using time-of-flight camera

The functionality of the ToF camera system was further investigated in a pseudoclinical scenario. The system was connected through a local area network and was accessed on a laptop for operator view and on a phone for "patient" view (feedback traces). The camera was installed on the LINAC couch to aim at the volunteer's chest/sternum area and the feedback phone provided live ROI movement traces as illustrated in Figure 4. BH, target, and ROI selection were set by the operator as required and the volunteer was asked to hold their breath accordingly as shown in Figure 5. Five volunteers of different ages and gender participated in this test and multiple traces were captured and recorded.

Results

Absolute accuracy

Absolute distance measurements are shown in Figure 6, where the blue dot represents the measured distances, the dashed orange line represents the ideal linear relationship, and the green line shows the expected relation between the measured and actual distance. The relationship was found to be nonlinear, as the light modulation is a square wave rather than sinusoidal as assumed in equation 1. This was because the light modulation generated by the TOF camera was square waves as mentioned in the manufacturer's specifications.

The results shown here are from test 1 as mentioned in the methods. There was negligible difference noticed in absolute

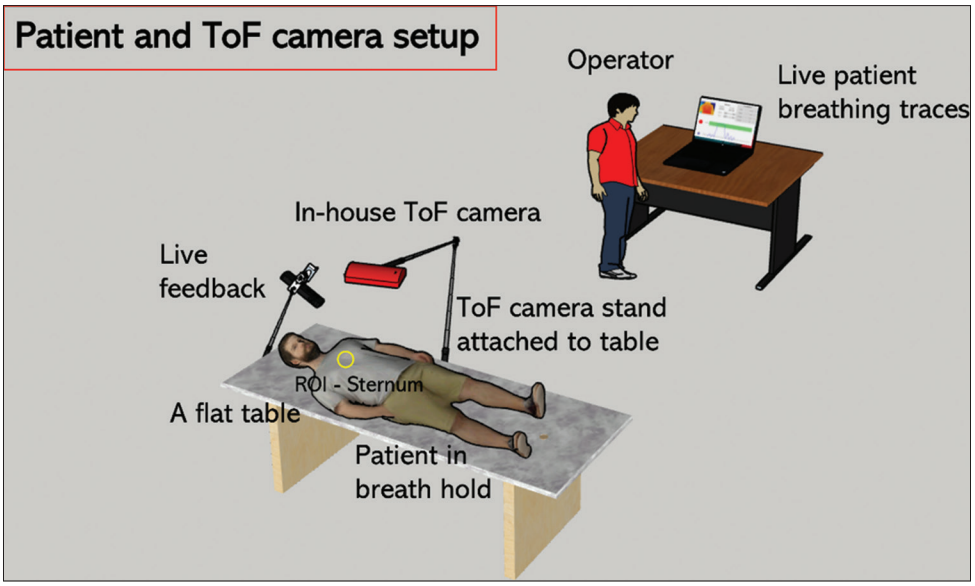

Figure 4: The schematic illustrates the patient and time-of-flight camera setup. TOF: Time-of-flight

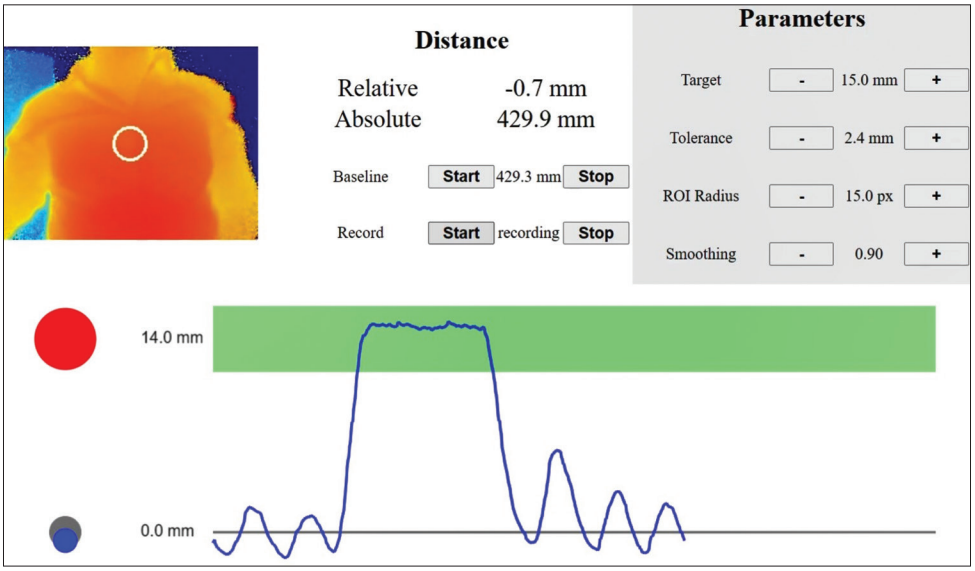

Figure 5: The web interface as seen by the operator

distances between these two tests. Test 2 was performed independently as a confirmation to rule out any setup inaccuracies in test 1.

Relative accuracy

The QUASAR phantom's motion traces are compared against the one measured with the ToF camera. The QUASAR phantom is placed at multiple distances away from the camera. The breath rate (15 bpm) is kept constant to minimize the dependency on the breath rate. The blue line is the camera-measured traces, and the orange dotted line is the expected curve for the settings as described in the methods. For the measurement performed at 30 cm away from the camera, it registered the 10 mm motion toward it as approximately 8 mm whereas the away motion was almost −10 mm.

In the case when the QUASAR phantom is placed 40 cm away, the camera has a better agreement with the expected as shown in Figure 7. The motion detected by the camera appears to be symmetric and is approximately 10 mm and-10 mm in each direction, respectively.

In addition to this, the camera is also tested for the effect of object tilt on the measurement. It is observed that a tilt as much as 5° does not have a significant impact on the surface measurement. The motion detected by the camera appears to be symmetric and is approximately 10 mm and − 10 mm in each direction, respectively.

Moreover, the camera is tested to investigate the effect of any lateral shift on the measurements. The QUASAR phantom is placed at the edge of the camera's field of view. The camera

appears to function as desired; however, it is noticed that the motion detected exceeded the expected 10 mm and −10 mm movement by marginal distance (<1 mm) in each direction, respectively. The intended camera alignment is normal to the ROI on the patient's surface, which will be emphasized during the training provided to radiation therapists (RTs). However, the effect of misaligned was tested to observe any variation in the result.

Response under different conditions

The effect of temperature on the camera's performance was tested. For the first 10 s, there was minimal deviation from the baseline (the camera is aimed at the selected ROI throughout the test). When a high temperature is detected by the camera, it starts to give deviation in the measured distance for the same selected ROI and varies in an almost linear fashion (varies up to 3 mm for 10 s of heat application). Upon the removal of heat, the response appears to be constant; however, it does not drop down to the preheat values.

The stability in the camera's response over time was also investigated. The camera was aimed at the ROI of an object to observe any deviation from the baseline. Due to noise, some minor fluctuations were observed; however, the average trend shows a constant response by the camera. The camera has a constant response through its usage, which is more than 30 min when tested. The expected camera on-time depends upon the number of patients to be coached. On average, it can be operational for 20–30 min per patient.

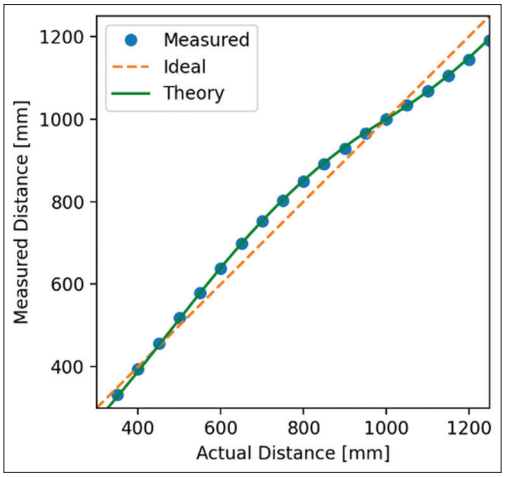

Figure 6: Absolute measurements with time-of-flight camera

Comparison with Elekta's active breathing coordinator

A BH comparison between Elekta's ABC and ToF surface camera is shown in Figure 8. The traces in red display the ToF camera detected sternum displacements (in mm) from the baseline. On the other hand, the blue lines represent the lung volume as measured by the ABC. It is observed that for the same 2 L BH lung volume, the surface motion of the subject varied in all three BHs. In the first and the third BH, the surface is seen to have a sudden rise in the beginning and it settles down as the subject tries to keep it in the threshold range (provided via feedback screen, directly over the subject's head). For the second BH, the trend observed for the surface motion is opposite and takes a few seconds to settle down. The comparison between the ABC system and the TOF camera is based on 5 volunteers' BH. The results are comparable, and Figure 8 is representative of the observed results.

Breath-hold tests using time-of-flight camera

Breathing traces of one of the five volunteers are illustrated in Figure 9. A tight tolerance of ±1 mm is selected to test the worst-case scenario to investigate how different age groups approach it. Maximum movement from the baseline is chosen based on the individual's lung capacity. In Figure 9, the blue line donates the volunteer's breathing traces and the red lines are the tolerance level. The ToF camera distance is the relative distance from the baseline and time is in seconds.

In the case of volunteer 1, the expected sternum movement is 15 mm within ±1 mm. The subject is only able to hold the breath partially in the first attempt and is out of the required position; however, improves it in the next attempts. It is also observed that sometimes the measurement is recorded beyond the maximum allowed tolerance.

Volunteer 2 BH measurements are shown in Figure 9. The expected movement in this case is 13 mm, which is chosen

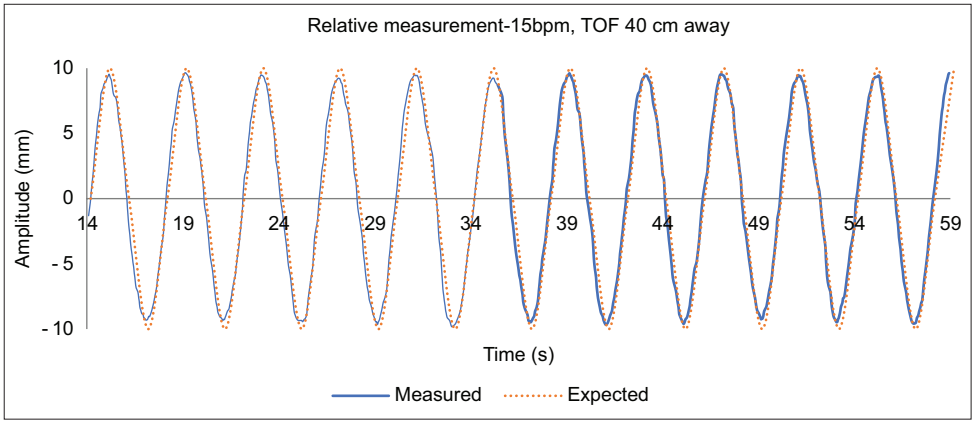

Figure 7: Relative measurement of QUASAR phantom operating at 15 bpm at 40 cm away, with time-of-flight camera. TOF: Time-of-flight

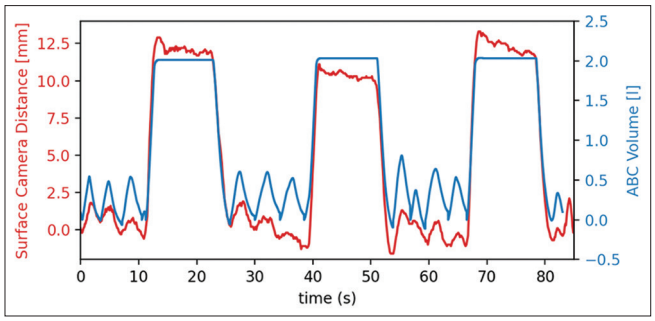

Figure 8: Breath-hold comparison of time-of-flight camera surface measurements and Elekta's active breathing coordinator lung volume. ABC: Active breathing coordinator

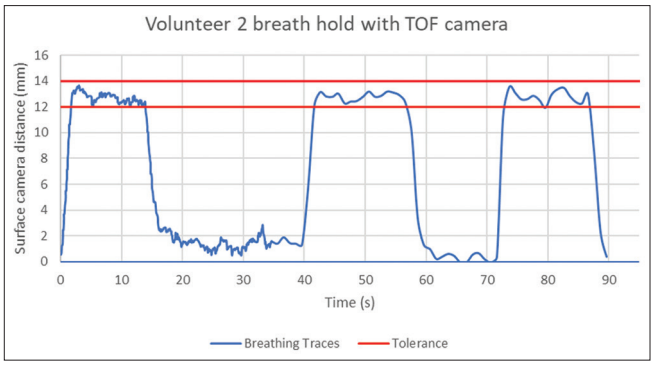

Figure 9: Volunteer 2 breath hold measurement using time-of-flight camera; expected movement in chest 13 mm anteriorly and tolerance of ± 1 mm. TOF: Time-of-flight

based on the measurement and trends observed in volunteer 1. The subject in this case is able to keep their breath constant and is within set tolerance in multiple attempts. In the case of volunteer 3, the desired sternum movement is 20 mm ± 1 mm. At the beginning of each BH attempt, the movement exceeds the tolerance and later stabilizes as the volunteer tries to follow the feedback provided by the overhead feedback phone. Volunteer 4 has an expected sternum movement of 10 mm ± 1 mm from the baseline. For the first two BH attempts, the movement either exceeded the tolerance or the subject was unable to hold their breath. In the third attempt, with some practice, the volunteer is able to maintain their breath within the desired limits. For volunteer 5 BH measurements, the desired sternum movement is 20 mm ± 1 mm. The first attempt results exceed the desired tolerance; however, an improvement is observed in the following attempts. Multiple attempts are performed to visualize the consistency in the camera following its usage for a longer period.

Discussion

Several tests were conducted to analyze the performance of a TOF camera for clinical application, aiming to coach external beam radiotherapy patients for BH treatments. The variation in absolute distance measurement was corrected by calibrating the camera at known distances. Although the primary requirement of the camera was relative measurements of the ROI, e.g., sternum, etc., the camera was also calibrated for absolute measurements. In addition to this, a calibrated QUASAR phantom was used to test the continuous surface tracking functionality and the measurement capabilities of the camera. It performed within ±2 mm when placed at distances beyond 40 cm away from the object. Measurements were also performed at an angle, and object placement was offset from the centerline. The camera has been designed to produce consistent results between 20 cm and 120 cm. Based on our results, we recommend operating the system at a 40-cm absolute distance, which also includes the benefit of covering the entire chest area of the patient that might be missed if placed too close. In addition to this, it is highly unlikely that the camera would be required to be positioned as far away as 120 cm for its current purpose.

In addition to this, the response of the camera was observed under different conditions. A sharp increase in response was seen when it was exposed to the temperature conditions of the order of ~400°C; however, it stabilized as soon as the heat source was removed. This demonstrates that the camera's response can vary if exposed to extreme temperatures. In the context of its BH application, the temperature in the clinic is maintained at an ambient level and it would have an insignificant effect on the performance. Moreover, relative distance is the distance between the camera and the baseline position of the ROI. Therefore, even if there is a slight deviation from ambient temperature, normalization of the measured signal to the initial readings would negate the effects due to minimal temperature changes. In addition, a test was performed to detect any startup effects, for which the camera was left on for a few minutes. The camera showed good consistency over the testing period. This illustrates that the camera does not require a warm-up period after it is turned on.

The TOF camera was tested simultaneously with Elekta's ABC, which is a well-established BH system, to correlate a patient's lung volume with surface motion. Three consecutive BHs were acquired to analyze the variation in the traces. It was observed that even though the lung volume is maintained constant by the ABC, the surface still has variation over the BH period. This could be attributed to the patient's body movement, given that no immobilization device was used, or it might have occurred in an effort to maintain the target volume. This can have dosimetric variations for the patients receiving radiation therapy for superficial tumor, e. g., breast cancer, and may require further investigation. In addition to this, the comparison with ABC indirectly relates the camera to patient coherent and is expected to be representative for cancer patients. However, a trial could be conducted with TOF camera on consented patients during their BH coaching with ABC before its clinical release.

In addition to this, the camera was tested on five volunteers with different BH capacities such as 10 mm, 13 mm, 15 mm, and 20 mm chest movement from the baseline with ±1 mm tolerance. The volunteers were able to hold their breath within the desired requirements with the aid of a feedback

module designed as part of the camera system. In our study, we observed that some subjects had difficulties holding their breath within a preset window, however, with some practice, the volunteers were able to accomplish the above requirement. This proves that our proposed system is able to coach the patient and achieve the desired outcome without consuming extra time on the imaging/treatment system. Volunteers were coached for BH using a feedback screen, as ExacTrac Dynamic provides the same interface for participants. No comparison of the reproducibility without the feedback screen was made as volunteers managed to follow their breathing movements without any external help. However, before the test, they were briefed about the functionality of the feedback screen and how it relates to their breathing pattern. All volunteers found the interface easy to follow and they were able to relate it to their breathing. From a clinical perspective, verbal feedback might complement the feedback screen as the current practice of BH with ABC uses verbal feedback. In addition to this, during treatment, RTs would be keeping a close look on BH in operator view and would be guiding the patients along with feedback screen.

A recent study published by Capaldi (2024) *et al*.[17] presented a couch-mounted smartphone-based motion monitoring system aimed at developing a cost-effective motion monitoring system for widespread implementation as an SGRT solution. Several recent papers have investigated the application of ToF cameras for contactless monitoring of respiration rate and tidal volume.[18-20] Our study differs from the above system in terms of utilization and accessibility. Our system is aimed at coaching patients for BH treatments which can be employed for multiple systems such as AlignRT, C-RAD, Identify, and/or Exactrac Dynamic. As a cost-effective coaching tool, our solution includes a patient feedback system that lets patients adjust their breathing patterns without minimal external assistance.

Conclusions

This study demonstrates the feasibility of using a cost-effective ToF camera to coach BH patients before imaging and/or treatment, releasing significant clinical time spent within the Linac bunker, or in imaging rooms. Our proposed coaching system is unique, cost-effective, accessible, and offers the flexibility to be operated in any room with a table or couch. We aim to integrate this system into our clinical workflow aiding in the improvement of BH compliance of patients undergoing DIBH for breast, liver, and lung cancers.

Financial support and sponsorship

Nil.

Conflicts of interest

There are no conflicts of interest.

References

1. Time of Flight (TOF) Camera for Raspberry Pi Arducam; 2023. Available from: https://www.arducam.com/time-of-flight-camera-raspberry-pi./[Last accessed on 2023 Apr 05].
2. Garibaldi C, Jereczek-Fossa BA, Marvaso G, Dicuonzo S, Rojas DP, Cattani F, *et al.* Recent advances in radiation oncology. Ecancermedicalscience 2017;11:785.
3. Debra M. Guidelines for using the ABC system on the elekta for respiratory gating treatment. Canc Therapy Oncol Int J 2018;9:555761.
4. RPM Respiratory Gating/RGSC (respiratory gating for scanners) on-site Training: Varian Home. Available from: https://www.varian.com/en-au/course/rpm-respiratory-gatingrgsc-respiratory-gating-scanners-site. [Last accessed on 2023 Apr 07].
5. Prabhakar R. Automatic verification of SSD and generation of respiratory signal with lasers in radiotherapy: A preliminary study. Phys Med 2012;28:43-7.
6. AlignRT® (2023) Vision RT. Available from: https://www.visionrt.com/align_rt/. [Last accessed on 2023 Apr 06].
7. Rad: Precision, Safety, and Efficiency in Advanced Radiation Therapy (2023) C. Available from: https://c-rad.com/. [Last accessed on 2023 Apr 06].
8. Identify Varian; 2023. Available from: https://www.varian.com/en-au/products/radiotherapy/real-time-tracking-motion-management/identify. [Last accessed on 2023 Apr 06].
9. EXACTRAC Dynamic® – A New Dimension in Patient Positioning and Monitoring. Brainlab; 2023. Available from: https://www.brainlab.com/radiosurgery-products/Exactrac/. [Last accessed on 2023 Apr 07].
10. Perrett B, Ukath J, Horgan E, Noble C, Ramachandran P. A framework for exactrac dynamic commissioning for stereotactic radiosurgery and stereotactic ablative radiotherapy. J Med Phys 2022;47:398-408.
11. Brandner ED, Chetty IJ, Giaddui TG, Xiao Y, Huq MS. Motion management strategies and technical issues associated with stereotactic body radiotherapy of thoracic and upper abdominal tumors: A review from NRG oncology. Med Phys 2017;44:2595-612.
12. Hamming VC, Visser C, Batin E, McDermott LN, Busz DM, Both S, *et al*. Evaluation of a 3D surface imaging system for deep inspiration breath-hold patient positioning and intra-fraction monitoring. Radiat Oncol 2019;14:125.
13. Seppenwoolde Y, Shirato H, Kitamura K, Shimizu S, van Herk M, Lebesque JV, *et al.* Precise and real-time measurement of 3D tumor motion in lung due to breathing and heartbeat, measured during radiotherapy. Int J Radiat Oncol Biol Phys 2002;53:822-34.
14. Geng J. Structured-light 3D surface imaging: A tutorial. Adv Optics Photonics 2011;3128.
15. Hansard M, Lee S, Choi O, Horaud R. Time-of-Flight Cameras, London, London Springer 2013; 978-1-4471-4657-5.
16. SPAD Depth Sensor for Automotive Lidar Applications: Products and Solutions Sony Semiconductor Solutions Group. Available from: https://www.sony-semicon.com/en/products/is/automotive/tof.html. [Last accessed on 2023 Apr 10].
17. Capaldi DP, Axente M, Yu AS, Prionas ND, Hirata E, Nano TF. A couch mounted smartphone-based motion monitoring system for radiation therapy. Pract Radiat Oncol 2024;14:161-70.
18. L'Her E, Nazir S, Pateau V, Visvikis D. Accuracy of noncontact surface imaging for tidal volume and respiratory rate measurements in the ICU. J Clin Monit Comput 2022;36:775-83.
19. Van Hove O, Andrianopoulos V, Dabach A, Debeir O, Van Muylem A, Leduc D, *et al.* The use of time-of-flight camera to assess respiratory rates and thoracoabdominal depths in patients with chronic respiratory disease. Clin Respir J 2023;17:176-86.
20. Guo K, Zhai T, Pashollari E, Varlamos CJ, Ahmed A, Islam MN. Contactless vital sign monitoring system for heart and respiratory rate measurements with motion compensation using a near-infrared time-of-flight camera. Appl Sci 2021;11:10913.